

Reactions of Cations Derived from Naphthalene with Molecules and Atoms of Interstellar Interest

Valéry Le Page,[§] Yeghis Keheyan,[†] Theodore P. Snow,[§] and Veronica M. Bierbaum[§]

Contribution from the Department of Chemistry and Biochemistry, and Center for Astrophysics and Space Astronomy, University of Colorado, Boulder, Colorado 80309, and Istituto di Chimica Nucleare del CNR, Monterotondo Stazione, 00016 Roma, Italy

Received September 30, 1998

Abstract: The chemistry of naphthalene radical cation and its derivatives ($C_{10}H_n^+$, $n = 6,7,8,9$) has been studied with molecules and atoms of interstellar interest in a selected ion flow tube. The radical cation $C_{10}H_8^+$ is unreactive with H_2 , CO , H_2O , and NH_3 but reacts with H , O , and N atoms. Adduct formation is the only channel detected in the case of reaction with H atoms, but additional channels contribute in reactions between $C_{10}H_8^+$ and O and N atoms; these latter reactions proceed through novel reaction pathways via C and CH abstraction, leading to the formation of the stable compounds CO and HCN , respectively. The closed-shell naphthyl cation $C_{10}H_7^+$ is essentially unreactive with atoms but associates via nucleophilic addition with most of the molecules studied. The reaction kinetics are close to saturation in the accessible helium pressure range. The naphthyl radical cation $C_{10}H_6^+$ does not react with H_2 , CO , or H_2O but forms an adduct with NH_3 at a moderate rate. Reactions with atoms were found to be very similar to those of $C_{10}H_8^+$. The implications of these results for the stability of polycyclic aromatic hydrocarbon cations in the interstellar medium are briefly discussed.

Introduction

Polycyclic aromatic hydrocarbons (PAHs) are thought to be important constituents of the interstellar medium (ISM) because of their ability to explain the unidentified infrared features (UIRs) between 3 and 13 μm .¹ These molecules might also contribute to the catalysis of molecular hydrogen,^{2–4} and, in their cationic form, they have been proposed as carriers of the diffuse interstellar bands (DIBs), which are absorption features in stellar visible spectra.^{5–7} Although they have not been unequivocally identified, evidence of PAH cations has been reported recently in a reflection nebula,⁸ based on the decreasing ratio of the 8.6–11.3 μm peaks with increasing distance from the illuminating star. This was attributed to changes in the relative populations of ionized and neutral molecules.

PAH cations are good candidates for carriers of the UIRs and DIBs due to their spectroscopic properties and their stability against photodissociation in strong UV fields. Experimental investigations have been carried out for the photochemistry of naphthalene, anthracene, and pyrene,^{9–12} as well as for larger

PAHs.^{13–15} However, there are few studies of the chemical reactivity of these species,^{16–18} particularly concerning their stability in the ISM. Herbst¹⁹ has pointed out that any precise evaluation of densities of PAH molecules in the ISM must await the experimental determination of the rate coefficients which govern the synthesis of these molecules in the gas phase. In this paper, our purpose is to assess these questions using naphthalene cation as a model of PAH cations. We have carried out experiments to examine the reactions of $C_{10}H_8^+$ with the most common species in the ISM^{20,21} namely H_2 and CO molecules, and H , N , and O atoms, which are believed to play a key role in the depletion of PAHs⁺. We also report results of reactions with the polar molecules H_2O and NH_3 . Due to the relative weakness of $C-H$ bonds compared to $C=C$ bonds, most large PAHs are thought to lose their peripheral hydrogen atoms before breaking the carbon skeleton in a UV field.^{22–24} A recent study of collision-activated dissociation of PAH cations contain-

(9) Ho, Y. P.; Yang, Y. C.; Klippenstein, S. J.; Dunbar, R. C. *J. Phys. Chem.* **1995**, *99*, 12115–12124.

(10) Gotkis, Y.; Oleinikova, M.; Naor, M.; Lifshitz, C. *J. Phys. Chem.* **1993**, *97*, 12282.

(11) Ling, Y.; Martin, J. M. L.; Lifshitz, C. *Int. J. Mass Spectrom. Ion Processes* **1997**, *160*, 39–48.

(12) Ling, Y.; Gotkis, Y.; Lifshitz, C. *Eur. Mass Spectrom.* **1995**, *1*, 41–49.

(13) Jochims, H. W.; Ruhl, E.; Baumgartel, H.; Tobita, S.; Leach, S. *Astrophys. J.* **1994**, *420*, 307–317.

(14) Allain, T.; Leach, S.; Seldmayr, E. *Astron. Astrophys.* **1996**, *305*, 602–615.

(15) Allain, T.; Leach, S.; Seldmayr, E. *Astron. Astrophys.* **1996**, *305*, 616–630.

(16) Bohme, D. K. *Chem. Rev.* **1992**, *92*, 1487–1508.

(17) Feng, W. Y.; Lifshitz, C. *Int. J. Mass Spectrom. Ion Processes* **1996**, *152*, 157–168.

(18) Nourse, B. D.; Cox, K. A.; Cooks, R. G. *Org. Mass Spectrom.* **1992**, *27*, 453–462.

(19) Herbst, E. *Astrophys. J.* **1991**, *366*, 133–140.

(20) Diplas, A.; Savage, B. D. *Astrophys. J.* **1994**, *427*, 274–287.

(21) Snow, T. P.; Witt, A. N. *Astrophys. J. Lett.* **1996**, *486*, L65–68.

(22) Léger, A.; Puget, J. L. *Astron. Astrophys.* **1984**, *137*, L5.

[§] University of Colorado.

[†] Istituto di Chimica Nucleare del CNR.

(1) Allamandola, L. J.; Tielens, A. G. G. M.; Barker, J. R. *Astrophys. Suppl. Ser.* **1989**, *71*, 733–775.

(2) Capron, L.; Mestdagh, H.; Rolando, C.; Sablier, M. *Proceedings of the 42nd ASMS Conference on Mass Spectrometry and Allied Topics*, Chicago, IL, May 29–June 3, 1994; pp 550–551.

(3) Cassam-Chenai, P.; Pauzat, F.; Ellinger, Y. In *Molecules and Grains in Space*; Nenner, I., Ed.; AIP Press: Woodbury, NY, 1994, p 543.

(4) Tielens, A. G. G. M. In *Dust and Chemistry in Astronomy*; Millar, T. J., Williams, T. A., Eds.; IOP Publishing: Philadelphia, PA, 1993; p 103.

(5) Crawford, M. K.; Tielens, A. G. G. M.; Allamandola, L. J. *Astrophys. J.* **1985**, *293*, L45–L48.

(6) Van der Zwet, G.; Allamandola, L. J. *Astron. Astrophys.* **1985**, *146*, 76–80.

(7) Léger, A.; d'Hendecourt, L. *Astron. Astrophys.* **1985**, *146*, 81–85.

(8) Joblin, C.; Tielens, A. G. G. M.; Geballe, T. R.; Wooden, D. H. *Astrophys. J.* **1996**, *460*, L119–L122.

ing from 10 to 24 carbon atoms confirms that C–H bond cleavage is favored over C=C bond cleavage.²⁵ Accordingly, dehydrogenated PAHs should play an important role in interstellar environments such as diffuse clouds, where the ionization field is strong.¹ Thus, we have extended the study of naphthalene cation to its dehydrogenated derivatives $C_{10}H_7^+$ and $C_{10}H_6^+$. Two isomers were detected in our study when these species were produced by reaction of $C_{10}H_8$ with He^+ ; therefore, we do not report quantitative results for the reactions of dehydrogenated naphthalene cations with atoms but do so only with molecules, where the extraction of the rate coefficients is somewhat more accurate. However, the lack of precise quantitative results does not affect our conclusions concerning the chemical stability of these compounds: due to the relatively fast reaction with H atoms, the most stable form of PAHs⁺ in the ISM are hydrogenated PAHs⁺.

Although $C_{10}H_8^+$ is not believed to be a major PAH in the ISM due to its lower stability against photodissociation, the chemistry of $C_{10}H_8^+$ with respect to the major neutrals, including H, H₂, CO, or O, is expected to be prototypical of larger PAHs⁺. Comparison with the chemistry of $C_6H_6^+$ where data are available, as in the case of reactions with H and H₂,^{26,27} or with our own experiments in the case of O and N atoms, supports this assumption.

Experimental Section

The major modifications of our selected ion flow tube (SIFT) apparatus were the addition of a cold cathode discharge to the source flow tube to produce rare gas metastable species and the connection of a microwave discharge tube to the reaction flow tube to form atomic reactants. The SIFT apparatus has been described in detail previously.²⁸ Briefly, ions are produced in the first flow tube, and then the ions of interest are selected using a quadrupole mass filter and injected into the second reaction flow tube through a venturi inlet, where the ions are entrained in helium. To ensure cooling of the ions and a stabilized laminar flow of the carrier gas, the first of the seven reactant inlets is situated 45 cm downstream from the venturi inlet. After reaction in the flow tube, the ions are detected using a second quadrupole mass filter and a channeltron electron multiplier.

$C_{10}H_8^+$ was formed by chemical ionization of naphthalene with He^+ and also by Penning ionization of naphthalene with argon metastables produced in a cold cathode discharge.²⁹ Typical conditions were as follows: argon flow, ~ 30 std $cm^3 s^{-1}$; voltage, ~ 270 V, biased so that electrons flow upstream in the discharge tube. This tube has an internal diameter of 12.7 mm, and the spacing between the two hollow cathodes is 20 mm. The voltage was kept as low as possible in order to prevent both the formation of $C_{10}H_7^+$ and a large production rate of Ar^+ . The power supplies connected to the source flow tube were modified to withstand the relatively high current produced by the hollow cathode discharge (over 15 mA instead of about 25 μA when the electron impact ionizer was used). The reaction between Ar^* and $C_{10}H_8$ is exothermic by 3.4 eV and is more likely to preserve the ring structure of naphthalene than when reaction with He^+ is used;³⁰ this latter reaction is exothermic by more than 16 eV. Production of naphthalene cation

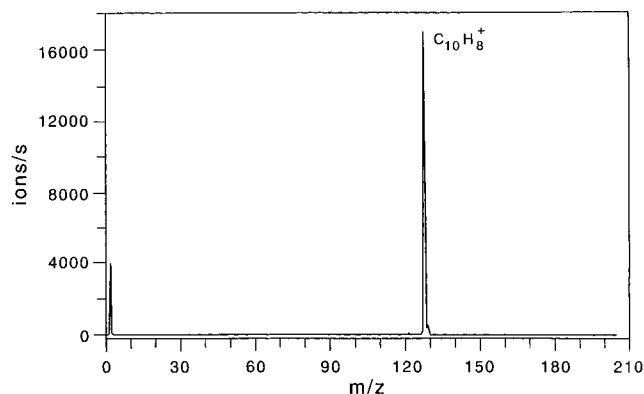


Figure 1. SIFT spectrum of $C_{10}H_8^+$ (mass 128) produced by the reaction of metastable argon with naphthalene. $^{13}CC_9H_8^+$ (mass 129) is present at a level of ~ 500 counts/s, while $C_{10}H_7^+$ (mass 127) is present at a level of 80 counts/s.

with the hollow cathode discharge was found to be very efficient, and count rates of cleanly selected $C_{10}H_8^+$ were up to 10^5 ions s^{-1} ; Figure 1 shows a SIFT spectrum of $C_{10}H_8^+$ generated in this manner. The dehydrogenated species $C_{10}H_7^+$ and $C_{10}H_6^+$ were formed by the reaction of He^+ or Ar^+ with naphthalene.

The pressure in the reaction flow tube was set to 0.5 Torr with a He flow of ~ 220 std $cm^3 s^{-1}$. The atoms were produced using a microwave discharge operating between 10 and 50 W. $N(^4S)$ atoms were formed in a pure nitrogen flow. Phosphoric acid coating of the discharge tube greatly enhanced the nitrogen atom density by preventing recombination on the walls, and dissociation ratios greater than 2% were observed. $O(^3P)$ atoms were produced using the well-known reaction $N + NO \rightarrow N_2 + O$.³¹ The titration was carried out using a mixture of 5.04% NO in He, and the flow rate was measured with a calibrated Tylan flowmeter. The O atom density in the reaction flow tube was as large as $5 \times 10^{12} cm^{-3}$. This method of O atom production was preferred over the direct formation of O atoms in a pure O₂ flow due to the possibility of producing reactive $O_2(^1\Delta_g)$ metastables.³² $H(^2S)$ atoms were formed in a similar way by flowing ultrahigh-purity H₂ through the microwave discharge tube. For all these reactants, no evidence for the production of more reactive metastable species was found. Calibration of the H atom density and estimation of the dissociation ratio were done using known reactions with H atoms.^{26,27,33} Dissociation ratios of the molecular hydrogen were up to 30% in pure H₂.³⁴ For production of N and H atoms, the parent gases were pure and not diluted by inert gases. The gas purities were as follows: helium buffer was commercial grade for the reactions with molecules and high purity (99.995%) for the reactions with atoms; prepurified argon (99.998%) from U.S. Welding was used for the hollow cathode discharge; N atoms were produced using UHP N₂ (99.999%) from U.S. Welding; conversion to O atoms was done using a mixture of 5.04% NO in He from Matheson; H atoms were produced using UHP H₂ (99.995%) from Air Products. Neutral reactants included trimethylamine (99.5%) from Matheson, CO (99.97%) from Specialty Gases Product Group, and NH₃ electronic grade (99.995%) from Air Products. H₂O vapor was produced using conventional distilled water.

(23) Allamandola, L. J.; Tielens, A. G. G. M.; Barker, J. R. *Astrophys. J.* **1985**, 290, L25.

(24) Tielens, A. G. G. M.; Allamandola, L. J.; Barker, J. R.; Cohen, M. In *Polycyclic Aromatic Hydrocarbons and Astrophysics*; Léger, A.; d'Hendecourt, L.; Boccaro, N., Eds.; Reidel: Dordrecht, The Netherlands, 1987; p 273.

(25) Wang, X.; Becker, H.; Hopkinson, A. C.; March, R. E.; Scott, L. T.; Bohme, D. K. *Int. J. Mass Spectrom. Ion Processes* **1997**, 161, 69–76.

(26) Petrie, S.; Javahery, G.; Bohme, D. K. *J. Am. Chem. Soc.* **1992**, 114, 9205–9206.

(27) Scott, G. B. I.; Fairley, D. A.; Freeman, C. G.; McEwan, M. J.; Adams, N. G.; Babcock, L. M. *J. Phys. Chem.* **1997**, 101, 4973–4978.

(28) Van Doren, J. M.; Barlow, S. E.; DePuy, C. H.; Bierbaum, V. M. *Int. J. Mass Spectrom. Ion Processes* **1991**, 109, 305–325.

(29) Howorka, F. *J. Chem. Phys.* **1978**, 68, 804.

(30) It is particularly important to use a gentle ionization process when forming small PAH cations such as $C_{10}H_8^+$. For example, when using He^+ rather than Ar metastables as an ionization agent, the reactivities of $C_6H_6^+$ and $C_{10}H_8^+$ toward nitrogen were found to be 80% and 65% lower, respectively; this suggests the formation of ring-opened isomeric ions when employing He^+ ionization. In addition, this can be seen as evidence that the ring structure in naphthalene is not destroyed when Ar metastables are used.

(31) Schiff, H. I. *Ann. Geophys.* **1964**, 20, 86.

(32) Schmitt, R. J.; Bierbaum, V. M.; DePuy, C. H. *J. Am. Chem. Soc.* **1976**, 101, 6443–6445.

(33) Tosi, P.; Ianotta, S.; Bassi, D.; Villinger, H.; Dobler, W.; Lindinger, W. *J. Chem. Phys.* **1984**, 80, 1905–1906.

(34) The dissociation ratio can be as high as 50% when using a mixture of H₂ and He. However, we use pure H₂ to avoid problems due to formation of helium metastables in the discharge.

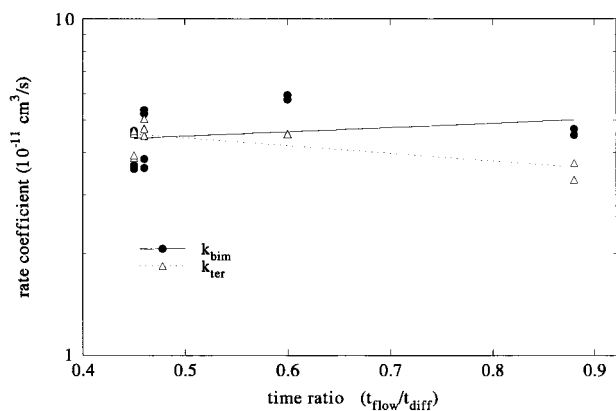


Figure 2. Measurements of the rate coefficient of the bimolecular reaction channel of the reaction between naphthalene cation and O atoms. The eight measurements at left were performed at four different pressures ranging from 0.5 to 0.8 Torr by decreasing the conductance of the valve between the flow tube and the roots blower, thus keeping the ratio $t_{\text{flow}}/t_{\text{diff}}$ constant (see text for details). These data show the reproducibility of the measurement. The four other measurements were performed at 0.3 and 0.4 Torr with the valve fully opened and a decreasing helium carrier flow. Consequently, the flow time increased and the diffusion time decreased, so the probability for an atom to reach the wall increased. There is no evidence of significant recombination on the flow tube walls.

Earlier estimates of the rate coefficients have shown that the effect of wall recombination of O atoms must be taken into account; we found that this effect is large when the wall is clean but slowly decreases to become negligible after O atoms have been flowing for an extended time. This observation is consistent with previous studies of different metallic surfaces, in which Sjolander found that the initial probability of O atom loss on clean surfaces was close to unity,³⁵ while after a few hours, the probability of loss decreased to an acceptable level. We found a similar effect in our study of the reaction between $\text{C}_{10}\text{H}_8^+$ and O atoms; the apparent rate coefficient was first found to be $\sim 75\%$ lower than the value reported in this paper. We also found that the ratio of the apparent rate coefficients for $\text{C}_{10}\text{H}_8^+ + \text{O}$ and $\text{C}_{10}\text{H}_8^+ + \text{N}$ slowly increased, and we interpret this effect as due to the larger reactivity of O atoms on the wall. After a while, the measured rate coefficient for reaction with O atoms reached a plateau, showing evidence for a less reactive wall. Determinations of the rate coefficients for both the bimolecular and the termolecular reaction channels were done under a variety of conditions to ensure that wall loss of O atoms was not occurring. To examine the effect of wall recombination, it is useful to compare the typical diffusion time, $t_{\text{diff}} (= \pi R^2/16D)$, where R is the flow tube radius and D is the diffusion coefficient of O atoms in helium, which is inversely proportional to helium pressure), to the total flow time, $t_{\text{flow}} (= L_{\text{flow}}/v)$, where L_{flow} is the distance between the atom inlet and the ion sampling orifice at the detection end and v is the average velocity of the helium buffer gas, which is proportional to helium flow rate and inversely proportional to helium pressure). This ratio $t_{\text{flow}}/t_{\text{diff}}$ is independent of pressure, and it is not possible to measure the wall effect by changing the pressure; however, the ratio depends on the helium flow, and thus decreasing the flow allows us to explore the reactivity of the wall toward O atoms. Figure 2 shows various measurements of the rate coefficient of the bimolecular reaction channel of the reaction between naphthalene cation and O atoms. The constancy of the bimolecular rate coefficient for a time ratio which varies by almost a factor of 2 for a given O atom flow indicates that, in this experiment, the influence of the wall is negligible.

The flow of O atoms alters the transmission of the sampling orifice (a molybdenum plate with a 1-mm-diameter hole at the detection end), thus giving an artificial lowering of the count rate as the NO titration reaction proceeds, leading to a possible overestimation of the rate coefficient. To account for this effect, we monitor the ratio between reactant and products as an indicator of the progress of the reaction.

(35) Sjolander, G. W. *J. Geophys. Res.* **1976**, *81*, 3767–3770.

We found no evidence of mass discrimination since the masses of the reactant and products are not very different.

Another problem arises from the fact that the reactants and the helium flow are not instantaneously homogeneously mixed. To estimate the magnitude of the mixing effect of O atoms in the flow tube, we have performed experiments at two different positions of the atom inlet (about 70 and 50 cm from the sampling orifice). Using the method previously described by Upschulte³⁶ (plotting the observed rate vs $1/z$ and then deducing the mixing distance from the intercept with the $1/z$ axis), we found evidence for a small mixing distance of about -5 cm, in good agreement with the known high diffusion coefficients of light atoms in helium.³⁷

For studies involving H atoms, we employ a calibration reaction, and, provided the wall effect is not large, the rate coefficient is directly deduced from the known rate and the ratio of reactivities. Therefore, incomplete mixing of reagents is not likely to affect the measurement of rate coefficients, and, in this case, all the experiments were carried out using the same position for the atom inlet. Use of the reaction between C_6H_6^+ and H as a calibration reaction is especially interesting because it gives directly the difference in reactivities of benzene and naphthalene cations and thus explores the effect of increasing size of PAH⁺ on its reactivity toward H atoms. We emphasize that there are two recent measurements of the rate coefficient of the reaction between benzene cation and atomic hydrogen which agree within 15%.^{26,27} Since the measurement of the rate coefficients between benzene cation and H atoms in the study of Scott et al.²⁷ was deduced from a calibration of the H density using the reaction between CO_2^+ and H, we also used this latter reaction when studying the chemistry between $\text{C}_{10}\text{H}_8^+$ and H.

Results and Discussion

Reactions with Molecules. (i) Reactions of $\text{C}_{10}\text{H}_8^+$ with Molecules. Before examining the reactivity of $\text{C}_{10}\text{H}_8^+$ with molecules of interstellar interest, it is important to demonstrate that only naphthalene ions, and no azulene ions, are present. We used the reaction previously described by Bohme et al.³⁸ between $\text{C}_{10}\text{H}_8^+$ and trimethylamine $(\text{CH}_3)_3\text{N}$ as a test for the presence of the azulene isomer in our studies. The reaction occurs via a charge-transfer process as reported in the study of Feng and Lifshitz.¹⁷ The ionization potential of trimethylamine is 7.83 eV, while the ionization potentials of naphthalene and azulene are 8.13 and 7.41 eV, respectively.³⁹ The reaction proceeds by fast charge transfer between $\text{C}_{10}\text{H}_8^+$ and trimethylamine occurring at or near the collision rate ($k_{\text{coll}} = 1.2 \times 10^{-9}$ cm^3/s); subsequent hydrogen transfer leads to protonated trimethylamine, which in turn adds with trimethylamine in the presence of He to give $(\text{CH}_3)_3\text{NH}(\text{CH}_3)_3\text{N}^+$. The series of reactions is as follows:

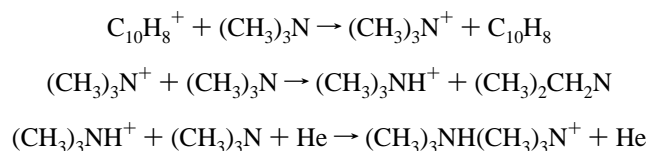


Figure 3 shows a typical plot for the reaction between $\text{C}_{10}\text{H}_8^+$ and $(\text{CH}_3)_3\text{N}$, with the reactant ion produced by Penning ionization of naphthalene with Ar^* . The absence of an unreactive component argues against the presence of azulene cations in the flow tube. We measured a rate coefficient for the charge-transfer reaction of 1.1×10^{-9} cm^3/s , in excellent agreement

(36) Upschulte, B. L. Ph.D. Thesis, University of Colorado, 1986.

(37) Morgan, J. E.; Schiff, H. I. *Can. J. Chem.* **1964**, *42*, 2300–2306.

(38) Bohme, D. K.; Wlodek, S.; Zimmerman, J. A.; Eyley, J. R. *Int. J. Mass Spectrom. Ion Processes* **1991**, *109*, 31–47.

(39) Lias, S. G.; Bartmess, J. E.; Liebman, J. F.; Holmes, J. L.; Levin, R. D.; Mallard, W. G. *J. Phys. Chem. Ref. Data* **1988**, *17*, Suppl. 1.

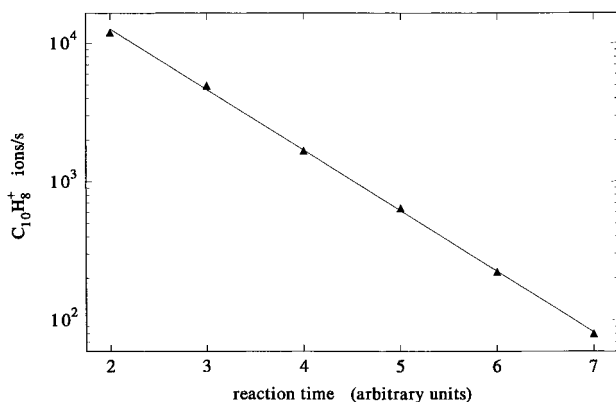


Figure 3. Typical plot for the reaction between $C_{10}H_8^+$ and $(CH_3)_3N$. The linearity of the semilogarithmic decay indicates that there is only one isomer.

Table 1. Rate Coefficients and Products for the Reactions of $C_{10}H_n^+$ ($n = 6, 7, 8, 9$) with Molecules

ionic reactant	molecular reactant	ionic products	rate coeff (cm^3/s) ^a
c- $C_{10}H_9^+$	H_2	—	no reaction ^b
	CO, H_2O, NH_3	—	no reaction ^c
c- $C_{10}H_8^+$	H_2, NH_3	—	no reaction ^b
	$CO, H_2O, N_2, O_2, NO,$ CH_3OH, CS_2	—	no reaction ^c
	$(CH_3)_3N$	$(CH_3)_3N^+$	1.1×10^{-9}
c- $C_{10}H_7^+$	H_2	$C_{10}H_9^+$	5.2×10^{-11} ^d
	CO	$C_{11}H_7O^+$	1.4×10^{-10} ^d
	H_2O	$C_{10}H_9O^+$	1.3×10^{-9} ^d
	NH_3	$C_{10}H_{10}N^+$	$\sim 5 \times 10^{-10}$ ^d
l- $C_{10}H_7^+$	H_2, CO, H_2O	—	no reaction ^c
	NH_3	$C_{10}H_{10}N^+$	$\sim 5 \times 10^{-10}$ ^d
c- $C_{10}H_6^+$	H_2	—	no reaction ^c
	CO, H_2O	—	no reaction ^c
	NH_3	$C_{10}H_9N^+$	2.9×10^{-11} ^d
l- $C_{10}H_6^+$	H_2, CO, H_2O	—	no reaction ^c
	NH_3	$C_{10}H_9N^+$	2.0×10^{-12} ^d

^a Rate coefficients are measured at 0.5 Torr of helium carrier pressure in the FA-SIFT experiments. Estimated total errors: $\pm 10\%$ for reaction with $(CH_3)_3N$; $\pm 15\%$ for reaction with H_2 ; $\pm 20\%$ for reactions with CO and H_2O ; and $\pm 30\%$ for reaction with NH_3 . ^b No products observed; $k < 5 \times 10^{-13} cm^3/s$. ^c No products observed; $k < 1 \times 10^{-12} cm^3/s$. ^d Termolecular association reaction.

with the values of Bohme et al.³⁸ ($1.1 \times 10^{-9} cm^3/s$) and of Feng and Lifshitz¹⁷ ($1.2 \times 10^{-9} cm^3/s$).

The $C_{10}H_8^+$ ions were found to be unreactive with H_2 , CO , NH_3 , H_2O , CS_2 , NO , and CH_3OH or at most slowly reactive; we report an upper limit of $10^{-12} cm^3/s$ for these reactions (except for H_2 and NH_3 , where the upper limit is $5 \times 10^{-13} cm^3/s$). Table 1 summarizes the results for all the reactions between ions and molecules. The reaction between $C_{10}H_8^+$ and NH_3 has also been studied by Feng and Lifshitz, and a rate coefficient of $5.3 \times 10^{-12} cm^3/s$ has been reported. These workers found an association reaction to form a product at mass 145. We have carried out new experiments on this reaction but consistently find an upper limit for the rate coefficient of about $5 \times 10^{-13} cm^3/s$, 1 order of magnitude below that of Feng and Lifshitz. A major problem arises from the presence of the adduct of $C_{10}H_7^+$ and H_2O at the same mass as the product reported by Feng and Lifshitz. When $C_{10}H_8^+$ is formed in the source by chemical ionization with He^+ , the exothermicity is sufficiently large to produce dehydrogenated species such as $C_{10}H_6^+$ and $C_{10}H_7^+$; we found, in fact, production of almost 50% $C_{10}H_7^+$ relative to $C_{10}H_8^+$ when using electron energies between 25 and 150 eV (a typical spectrum is shown in Figure 4). This causes two main problems. First, there is always contamination

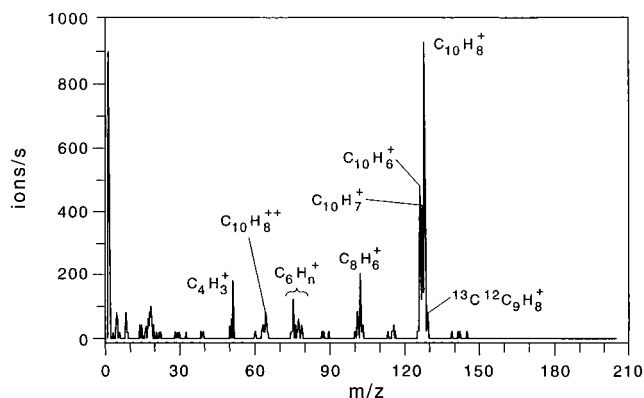


Figure 4. Spectrum of the products of the reaction between He^+ and $C_{10}H_8$ before selection of the reactant ion using the SIFT mass filter. The peak at mass 129 is $\sim 11\%$ of the $C_{10}H_8^+$ signal intensity due to the natural abundance of ^{13}C in naphthalene. The intensity of the doubly charged cation $C_{10}H_8^{2+}$ is low for EI at 50 V (this figure) but increases dramatically with increasing energy of the electrons.

of $^{13}C^{12}C_9H_7^+$ in the main peak of $C_{10}H_8^+$ (about 11% of the intensity of $C_{10}H_7^+$). Therefore, in our case this contribution is about 5% of the total $C_{10}H_8^+$ intensity and is almost independent of the electron energy. The second problem arises from the difficulty of injecting $C_{10}H_8^+$ at mass 128 without traces of $C_{10}H_7^+$ at mass 127 even at high resolution; therefore, in our experiments which use He^+ as the precursor ion, we always injected $C_{10}H_7^+$ at the level of a few percent. Thus, for the reaction $C_{10}H_8^+ + NH_3$, the product at mass 145 can be a mixture of three ions: $C_{10}H_8NH_3^+$, the adduct with naphthalene cation; $C_{10}H_7H_2O^+$, the adduct due to the fast reaction between naphthylum cation and water impurities; and $^{13}C^{12}C_9H_7NH_3^+$, arising from the contamination of the $C_{10}H_8^+$ peak with carbon-13. To avoid these problems, we studied the reaction of $^{13}C^{12}C_9H_8^+ + NH_3$, and we produced $C_{10}H_8^+$ using argon metastables; however, we did not observe any product at mass 146, which would correspond to the adduct of $^{13}C^{12}C_9H_8^+$ and ammonia. Consequently, in this study, we report an upper limit for this reaction rate constant of $5 \times 10^{-13} cm^3/s$.

What might explain the discrepancies between the two studies is the possibility of forming an excited, more reactive form of naphthalene cation when producing $C_{10}H_8^+$ by electron impact. Bohme et al. have reported³⁸ that when $C_{10}H_8^+$ is produced by electron impact on naphthalene, a small fraction ($< 5\%$) reacts with C_2H_2 to produce $C_{12}H_9^+ + H$; this reaction was attributed to an excited form of naphthalene cation. This channel was not seen when $C_{10}H_8^+$ was produced in a more gentle way, such as chemical ionization with Si^+ , a reaction with an exothermicity of only 0.01 eV, and consequently not likely to form $C_{10}H_8^{*+}$.

(ii) Reactions of $C_{10}H_7^+$ and $C_{10}H_9^+$ with Molecules. The semilogarithmic plot of the count rate of the dehydrogenated naphthalene cations, $C_{10}H_7^+$ and $C_{10}H_6^+$, versus neutral density shows the presence of two isomers, and therefore the rate coefficients are deduced from a two-exponential fit (an example with $C_{10}H_6^+$ is shown in Figure 5). The tail corresponding to the less reactive isomer is fitted first, and then the larger rate constant is deduced from the difference (a direct two-exponential fitting of the plot was found to be unsatisfactory when using either the Marquardt–Levenberg algorithm⁴⁰ or the simplex method). This is similar to the case of phenylum ions, where the presence of two isomers of different reactivities has been reported.^{41–43} Ausloos et al.⁴⁴ have noted that, when $C_6H_5^+$ is formed by charge-transfer-induced fragmentation of chloroben-

(40) Marquardt, D. W. *J. Soc. Ind. Appl. Math* **1963**, *2*, 431–441.

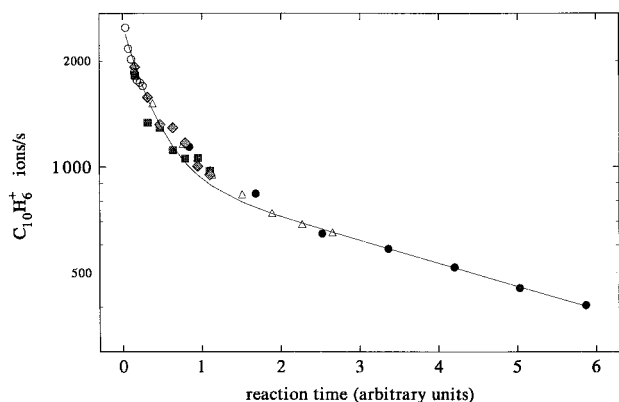
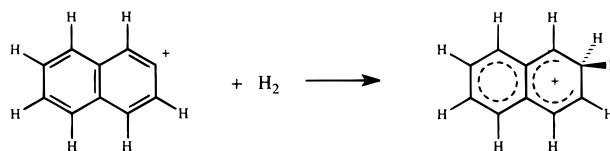


Figure 5. Plot of $C_{10}H_6^+$ versus reaction time. One can see the presence of two isomers with different reactivities.

zene with Kr^+ (IP = 14 eV), no unreactive ions were observed, but an appreciable fraction ($\sim 20\%$) was observed when using Ar^+ (IP = 15.8 eV). Consequently, an energy barrier of ~ 2.0 eV to ring opening was deduced for the formation of $l-C_6H_5^+$ from chlorobenzene, since the threshold for the formation of phenylum cation from chlorobenzene is only 12.47 eV.³⁹ In the case of chemical ionization of naphthalene with He^+ , the two isomers were produced in approximately equal amounts (with $\sim 8\%$ more of the reactive isomer at 0.5 Torr). To be certain that the two-exponential decays were due to the presence of two different isomers and not due to the presence of a more reactive excited species, we have carried out five experiments at helium pressures of 0.5, 0.6, 0.7, 0.8, and 0.9 Torr, each time measuring the ratio of the isomers versus the total counts. The amount of the unreactive isomer was found to be bracketed in the range between 46 and 51.5% with a small increase with increasing pressure in the flow tube. This small dependence of the ratio on He pressure could be due to a small difference in the diffusion coefficients of the two isomers. Although He is known to be a poor quencher,⁴⁵ the analysis of these data in terms of a quenching process for $C_{10}H_7^{+*}$ in helium would lead to a quenching rate of the excited species of about 3×10^{-16} cm³/s, which appears to be a very slow rate for the relatively large $C_{10}H_7^+$ ion (additionally, the amount of unreactive isomer is found to be the same even when using an excess of the polar molecules H_2O or NH_3 , which are known to be very good quenchers⁴⁵). Moreover, in the case of phenylum cation, the fact that the unreactive population did not decrease after the ions had undergone more than 100 collisions with aromatic molecules led Ausloos et al. to suggest the existence of an isomeric form rather than an excited state.⁴⁴ Therefore, we interpret the two-exponential decay as evidence for the formation of two isomers. Production of the ions using He^+ does not allow us to assign the two isomers since the exothermicities involved in the production of the two ions are not sufficiently different to produce one species selectively. The heat of formation of $C_{10}H_7^+$ at 300 K has been recently estimated to be about 275 ± 3 kcal/mol in a TPIMS/TRPD experiment (time-resolved photoionization mass spectrometry/time-resolved photodissociation);⁴⁶ thus, the reaction of Ar^+ with naphthalene to form $C_{10}H_7^+$ is exothermic by only 3.1 eV. To assign the reactive

and “unreactive” isomers as cyclic or acyclic forms of the molecule, we have performed an experiment where $C_{10}H_7^+$ was produced by reaction with Ar^+ . By using this gentle ionization process, the “unreactive” species was reduced to only about 20–25% of the total $C_{10}H_7^+$ signal. Thus, we assign the cyclic structure to the reactive isomer and the acyclic structure to the less reactive species.

$c-C_{10}H_7^+$ is a strong electrophile due to the presence of a vacant sp^2 orbital at the reactive site. For all reactions, the observed primary product is association between $c-C_{10}H_7^+$ and the neutral, as in the case of the reaction between naphthylum ion and molecular hydrogen, for example:



The rate coefficients depend strongly on the dipole moment and polarizability of the neutral. Table 1 shows that the association reaction is very efficient for water ($k_{obs}/k_{coll} = 3/4$),⁴⁷ while the efficiency is as low as 3.5% for H_2 . In the association reactions with water, we have seen adducts $C_{10}H_7^+(H_2O)_n$ up to $n = 2$, while for NH_3 the addition is more efficient and adducts up to $n = 4$ were observed. We have also observed the formation of NH_4^+ as a secondary product, which in turn gave adducts with ammonia up to $n = 3$. Moreover, when producing $C_{10}H_9^+$ directly in the source by reacting $C_{10}H_7^+$ with H_2 and injecting this ion into the reaction flow tube, we have seen the rapid formation of NH_4^+ due to the reaction $C_{10}H_9^+ + NH_3 \rightarrow NH_4^+ + C_{10}H_8$. In contrast, CO and H_2O were found to be unreactive with $C_{10}H_9^+$. This is due to the high proton affinity (PA) of NH_3 relative to that of $C_{10}H_8$ (204 vs 194.4 kcal/mol⁴⁸), while the PAs of H_2O and CO are only 166.5 and 141.9 kcal/mol, respectively. If $C_{10}H_9^+$ were an ionic complex, then the heat of formation would be $\Delta H_f^\circ(C_{10}H_9^+) = \Delta H_f^\circ(C_{10}H_7^+) - BDE$, where BDE is the bond energy of the ionic complex. Thus, the enthalpy of the reaction $C_{10}H_7 \cdot H_2^+ + H_2O \rightarrow C_{10}H_8 + H_3O^+$ would be $\Delta H = (-40 + BDE)$ kcal/mol (using a value of 275 kcal/mol for $\Delta H_f^\circ(C_{10}H_7^+)$ at 300 K derived from Gotkis et al.⁴⁶); the reaction is likely to be exothermic due to the typically low bond energy of ionic complexes (~ 15 – 20 kcal/mol). On the contrary, assuming a covalent structure for $C_{10}H_9^+$ leads to an endothermicity for the reaction of more than 1 eV. Consequently, the absence of reaction with CO and H_2O argues in favor of a covalently bonded structure for $C_{10}H_9^+$. An adduct ion is also formed by the reaction $C_{10}H_7^+ + NH_3$, which then produces NH_4^+ by the secondary reaction $C_{10}H_7NH_3^+ + NH_3 \rightarrow NH_4^+ + C_{10}H_7NH_2$. This latter reaction suggests that the PA of naphthalenamine is lower than the PA of ammonia. These values are expected to be similar since the PA of aniline, $C_6H_5NH_2$, is very close to that of ammonia. However, the reaction may be slightly endothermic and still occur if the $C_{10}H_7NH_3^+$ is not collisionally cooled before further reaction with NH_3 . It is also possible that the NH_4^+ ion is formed exclusively by the $l-C_{10}H_7^+$ isomer, whose thermochemistry is poorly known.

(41) Eyler, J. R.; Campana, J. E. *Int. J. Mass Spectrom. Ion Processes* **1983**, *55*, 171–178.

(42) Giles, K.; Adams, N. G.; Smith, D. *Int. J. Mass Spectrom. Ion Processes* **1989**, *89*, 303–317.

(43) Knight, J. S.; Freeman, C. G.; McEwan, M. J.; Anicich, V. G.; Huntress, W. T. *J. Phys. Chem.* **1987**, *91*, 3898–3902.

(44) Ausloos, P.; Lias, S. G.; Buckley, T. J.; Rogers, E. E. *Int. J. Mass Spectrom. Ion Processes* **1989**, *92*, 65–77.

(45) Ferguson, E. E. *J. Phys. Chem.* **1986**, *90*, 731–738.

(46) Gotkis, Y.; Naor, M.; Laskin, J.; Lifshitz, C.; Faulk, J. D.; Dunbar, R. C. *J. Am. Chem. Soc.* **1993**, *115*, 7402–7406.

(47) k_{coll} , the gas kinetic collision rate coefficient, is calculated using the ADO model: Su, T.; Bowers, M. T. In *Gas-Phase Ion Chemistry*; Bowers, M. T., Ed.; Academic Press: New York, 1979; Vol. 1, pp 83–118.

(48) Meot-Ner (Mautner), M.; Sieck, L. W. *J. Am. Chem. Soc.* **1991**, *113*, 4448–4460.

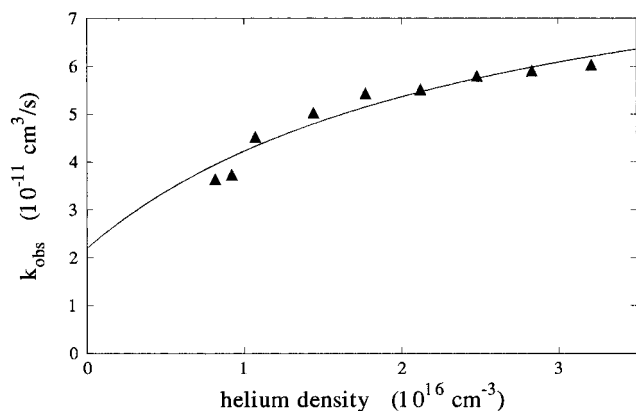


Figure 6. Plot of the observed bimolecular rate coefficient of the reaction between $c\text{-C}_{10}\text{H}_7^+$ and H_2 versus the helium density in the flow tube. From the fit, a lifetime of about 1×10^{-7} s is deduced for the intermediate tight complex. The following formula is used in this analysis: $k_{\text{exp}} = k_{\text{rad}} + rk_{\text{coll}}k_s[M]/(k_b + k_s[M])$, where k_{exp} is the measured rate, k_{rad} is the radiative rate (from ICR experiments), r is the ratio between the expected saturated rate and the observed rate, k_{coll} is the rate of complex formation, k_s is the rate of stabilization, $[M]$ is the carrier gas density, and k_b is the unimolecular rate of complex redissociation, from which the lifetime is directly deduced.

The chemistry of phenylium cation, C_6H_5^+ , with H_2O and NH_3 has recently been investigated by Ranasinghe and Glish,⁴⁹ and, in the case of H_2O , the exclusive product is also the adduct. Their MOPAC calculations in the case of H_2O and NH_3 favor structures with a single bond between the reactive site and the O or N atom. These experiments were performed in a quadrupole ion trap at low pressure, and, in the case of the reaction of C_6H_5^+ with NH_3 , they also reported a 10% association channel, with H atom loss leading to $\text{C}_6\text{H}_7\text{N}^+$. We do not observe the corresponding channel in the reaction $c\text{-C}_{10}\text{H}_7^+ + \text{NH}_3$, but the higher number of degrees of freedom (57 instead of 39) allows greater randomization of the available energy.⁵⁰ We cannot rule out this channel completely; in fact, we do observe a product at mass 143 but believe this ion arises from reaction between $\text{C}_{10}\text{H}_6^+$ and NH_3 ($\text{C}_{10}\text{H}_6^+$ is present at $\sim 2\%$ of the $\text{C}_{10}\text{H}_7^+$ intensity). Ranasinghe and Glish have not investigated the kinetics of reactions of phenylium cation with water and ammonia, but there are a few related measurements in the literature for reactions between $c\text{-C}_6\text{H}_5^+$ and H_2 and CO . The reactivity of $c\text{-C}_{10}\text{H}_7^+$ seems to be very close to that of $c\text{-C}_6\text{H}_5^+$. For the reaction with H_2 reported here, the rate coefficient of 5.2×10^{-11} cm^3/s is similar to that found for C_6H_5^+ in two previous studies,^{26,42} while the rate coefficient for the association with CO is found to be 30% lower for $\text{C}_{10}\text{H}_7^+$ than the value reported by Giles et al.⁴² for C_6H_5^+ . Such comparisons are useful in exploring the dependence of reactivity on the size of the PAH cation.

We have carried out experiments on the pressure dependence of the rate constant for reactions between $c\text{-C}_{10}\text{H}_7^+$ and H_2O and H_2 , which are two limiting cases. For H_2 , k_{obs} increases with pressure, as shown in Figure 6. In contrast, the observed rate constant for reaction of $c\text{-C}_{10}\text{H}_7^+$ with H_2O shows no pressure dependence in the accessible range of helium densities;

(49) Ranasinghe, Y. A.; Glish, G. L. *J. Am. Soc. Mass Spectrom.* **1996**, *7*, 473–481.

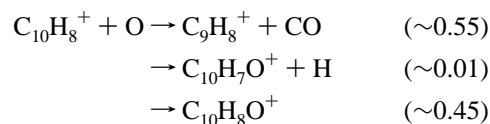
(50) Another reason may be the lack of collisional stabilization of the excited $\text{C}_{10}\text{H}_7\text{NH}_3^+$ ion in the ICR experiments. If the lifetime of the excited complex is greater than the collision time with He in the SIFT (typically 10^{-7} s), then the complex might be stabilized before entering the H loss channel; this would explain the restriction of available channels in SIFT experiments.

therefore, we report a lower limit for the termolecular association coefficient of about 10^{-26} cm^6/s . Such a high rate is not surprising, and even higher rates have been reported, for example, in the association of small electrophilic species with water (for example, $\text{CH}_3^+ + \text{H}_2\text{O}$, where k_{ter} is reported to be greater than 3×10^{-26} cm^6/s).⁵¹ This is probably due to the strong bond in the complex, which is formed by interaction between the vacant orbital of the ion and a lone pair of the reactant during the nucleophilic addition. The case of association with H_2 is more interesting; our pressure studies indicate that experiments were carried out in the “falloff” regime and allow us to deduce a lifetime for the $\text{C}_{10}\text{H}_9^{+*}$ complex of about 1×10^{-7} s. It is intriguing that the observed rate coefficient, while close to the saturation regime, lies far below the expected collision rate of about 10^{-9} cm^3/s ; one expects to approach this value as the helium density increases since the collision time becomes smaller than the lifetime of the complex, and each collision between the ion and the reactant is likely to stabilize the system. This behavior has been reported previously in studies of smaller hydrocarbons with H_2 but seems to occur preferentially in larger systems. These results can be interpreted as being due to the existence of two complexes.^{42,52,53} In this interpretation, the cation and the reactant first form a loose orbiting complex which can decay back to the reactant or lead to the formation of a second tight complex; this second complex can then be stabilized by collision with the buffer or return to the loose complex. If this hypothesis is correct, then our deduced lifetime applies to the second tight complex, and the efficiency ($k_{\text{obs}}/k_{\text{coll}}$) gives the ratio between the two exit channels for the first loose electrostatic complex toward reactants or toward the second covalent complex.

(iii) Reactions of $c\text{-C}_{10}\text{H}_6^+$ with Molecules. The $c\text{-C}_{10}\text{H}_6^+$ cation shows an intermediate reactivity, lying between those of $c\text{-C}_{10}\text{H}_7^+$ and $\text{C}_{10}\text{H}_8^+$. This behavior has been seen previously by Nourse et al.¹⁸ in their study of pyrene cation and its dehydrogenated derivatives. $\text{C}_{10}\text{H}_6^+$ is unreactive with H_2 , CO , and H_2O . Reaction occurs only with NH_3 , and the main product is the adduct $\text{C}_{10}\text{H}_6\text{NH}_3^+$, which in turn reacts to form $\text{C}_{10}\text{H}_6(\text{NH}_3)_2^+$ and $\text{C}_{10}\text{H}_6(\text{NH}_3)_3^+$. We find no evidence for the formation of NH_4^+ in the reaction $\text{C}_{10}\text{H}_6\text{NH}_3^+ + \text{NH}_3 \rightarrow \text{C}_{10}\text{H}_7\text{-NH} + \text{NH}_4^+$, probably due to the expected large heat of formation of the radical $\text{C}_{10}\text{H}_7\text{NH}$. The small NH_4^+ peak is believed to arise from secondary reactions of trace amounts of injected $\text{C}_{10}\text{H}_7^+$.

Reactions with Atoms. The reactions of naphthalene cations with atomic reactants display dramatically different behavior. For these systems, the most reactive species are $\text{C}_{10}\text{H}_8^+$ and $\text{C}_{10}\text{H}_6^+$ (see Table 2). The naphthylum cation shows almost no reactivity toward atoms; the only significant reaction for this species is with H atoms. The lack of reactivity of $\text{C}_{10}\text{H}_7^+$ is interpreted as being due to the absence of an unpaired electron which can readily bond with another unpaired electron in the atom. $\text{C}_{10}\text{H}_9^+$ is essentially unreactive with H, N, and O atoms.

(i) Reactions of $\text{C}_{10}\text{H}_n^+$ with O and N Atoms. The reaction between $\text{C}_{10}\text{H}_8^+$ and O atoms proceeds in the following way:



(51) Adams, N. G.; Smith, D. *J. Phys. B* **1976**, *9*, 1439.

(52) Neilson, P. V.; Bowers, M. T.; Chau, M.; Davidson, W. R.; Aue, D. H. *J. Am. Chem. Soc.* **1978**, *100*, 3649–3658.

(53) Smith, D.; Adams, N. G. *Int. J. Mass Spectrom. Ion Processes* **1987**, *76*, 307.

Table 2. Rate Coefficients and Products for the Reactions of $C_{10}H_n^+$ ($n = 6, 7, 8, 9$) with Atoms

ionic reactant	atomic reactant	ionic products (branching ratio)	rate coeff (cm ³ /s) ^a
$C_{10}H_9^+$	H	c- $C_{10}H_{10}^+$	$\sim 4 \times 10^{-12}$
$C_{10}H_8^+$	H	$C_{10}H_9^+$ (1.0)	1.9×10^{-10}
	O	$C_9H_8^+$ (0.55) ^b $C_{10}H_8O^+$ (0.45) ^b	1.0×10^{-10}
$C_{10}H_7^+$	N	$C_9H_7^+$ (0.3) ^b $C_{10}H_8N^+$ (0.7) ^b	2.3×10^{-11}
	H	$C_{10}H_8^+$ (1.0)	$\leq 5 \times 10^{-11}$
	O	—	$< 2 \times 10^{-11}$
$C_{10}H_6^+$	N	—	$< 1 \times 10^{-11}$
	H	$C_{10}H_7^+$	$\sim 2 \times 10^{-10}$ ^c

^a Represents reactivity of cyclic reactant ion, unless otherwise specified. Estimated total errors: $\pm 20\%$ for reactions of O atoms; $\pm 30\%$ for reactions of N atoms; $\pm 30\%$ for reactions of H atoms with $C_{10}H_8^+$; and $+100/-50\%$ for reaction between c- $C_{10}H_9^+$ and H atoms. Helium pressure is 0.5 Torr. Adducts are formed by termolecular association. ^b Estimated error: $\pm 10\%$. ^c Reactivity due to both cyclic and acyclic reactant ions.

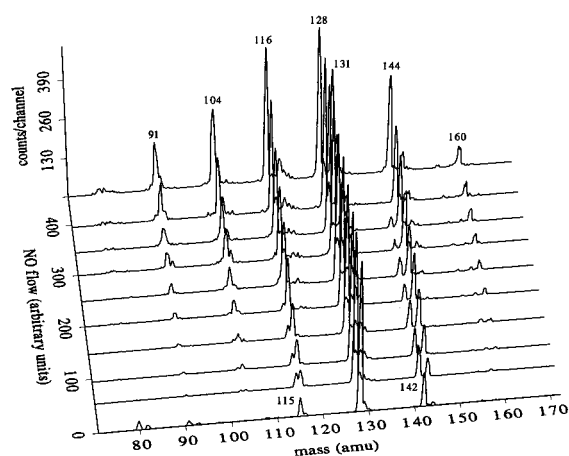
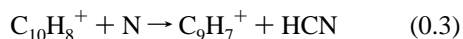


Figure 7. Reaction of $C_{10}H_8^+$ with N atoms and O atoms. As the NO flow is increased, N atoms are converted to O atoms; therefore, the products of the reaction of $C_{10}H_8^+$ with N disappear (masses 115 and 142), and the products of the reaction of $C_{10}H_8^+$ with O increase (primary products at masses 116 and 144 and other products from secondary reactions). The measured NO flow at the endpoint gives directly the flow rate of atoms.

For the first channel to be exothermic, the enthalpy of formation of the $C_9H_8^+$ product must be below 309.4 kcal/mol; thus, the structure of the product could be that of indene cation ($\Delta H_f^\circ = 226.7$ kcal/mol) or the radical cations of vinyltoluene (263.5 kcal/mol) or propynylbenzene (258.2 kcal/mol). The lack of reaction of $C_{10}H_7^+$ with atoms argues against the formation of ionic complexes, and therefore we believe that $C_{10}H_8O^+$ has a covalently bonded structure.

Figure 7 shows the products of the reaction of $C_{10}H_8^+$ with a fixed nitrogen atom production rate but at variable NO flows. Consequently, the first spectrum shows the products of the reaction between $C_{10}H_8^+$ and N, while the last spectrum shows the products of the reaction between $C_{10}H_8^+$ and O atoms (see Figure 8). We found the reaction between $C_{10}H_8^+$ and N atoms to proceed by both association and CH abstraction:⁵⁴



In contrast to the reaction with O atoms which produces different secondary products, the reaction with N is limited to the two primary species (Table 3). This is probably because the reactions

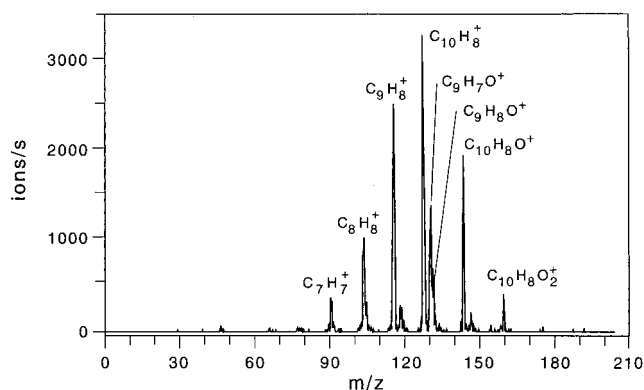


Figure 8. Products of the reaction between $C_{10}H_8^+$ and O atoms. The two primary products are at masses 116 and 144. Secondary reactions produce ions at masses 91, 104, 105, 131, 132, and 160. The flow rate of NO is ~ 0.05 std cm³ s⁻¹.

between $C_{10}H_8^+$ and N (and also H atoms) lead to the loss of radical character and, as the products are simple cations, they behave much like $C_{10}H_7^+$, which is relatively unreactive toward atoms.⁵⁵ The main products in the case of reaction between $C_{10}H_8^+$ and O are the adducts ($C_{10}H_8O^+$ and $C_{10}H_8O_2^+$); the lighter species arise from C or CH abstraction ($C_9H_8^+$, $C_8H_8^+$, $C_7H_7^+$), and $C_9H_8O^+$ could arise from either $C_{10}H_8O^+$ or $C_9H_8^+$ (however, we found experimentally that the addition between indene cation $C_9H_8^+$ and O atoms is not very efficient). The reactivity of $C_{10}H_6^+$ toward atoms is very similar to that of $C_{10}H_8^+$, and Figure 9 shows this similarity for reaction with O atoms. After the first reaction with an O atom, it is probable that the radical and the charge of both $C_9H_8^+$ and $C_9H_6^+$ are now localized on the remaining benzene ring, allowing the reaction to proceed a second time in the same way. The last reaction proceeds with CH abstraction (masses 89 and 91), leading to the loss of radical character. Therefore, it is not surprising to see an accumulation of the product at mass 91 at long reaction time (see Figure 10) between $C_{10}H_8^+$ and O. This last reaction of CH abstraction can be simply interpreted if both preceding reactions occur by ring-opening, leading to species that terminate with C-H (after possible hydrogen shifts). Therefore, one additional reaction with O atom may cleave the molecule at a terminal C-C bond of a chain, thus leading to the formation of HCO. The presence of masses 91 and 92 (the latter probably more reactive and thus less intense) can be explained if the first reaction opens the benzene ring. Nevertheless, another possibility which may explain the product at mass 91 is the formation of the stable aromatic tropylium ion by cleavage of the central bond in $C_8H_8^+$, and thus we cannot rule out the presence of an indene-like structure for the primary product. Indeed, as described in the next section, a consideration of the energetics of the reactions supports a ring structure for $C_9H_8^+$.

The earlier studies of substituted PAHs molecules by Beynon et al.⁵⁶ have shown that molecules such as phenol, naphthols, or anthraquinone, when ionized and excited by electron impact, are subject to CO and sometimes HCO losses. This is due to

(54) Although both isomeric forms HCN and HNC can be produced in this reaction, ab initio calculations in the case of $C_6H_6^+ + N$ favor the formation of a C-N bond over an insertion process in a C-H bond for the adduct; thus, the assignment of HCN for the neutral product is preferred.

(55) Calculations using the Gaussian 94 package indicate a singlet ground state for the c- $C_{10}H_7^+$ cation. A complete geometry optimization was performed for each state at the ROHF/6-31G* level, followed by a single-point calculation at the MP3 level with the 6-31G* basis set.

(56) Beynon, J. H.; Lester, G. R.; Williams, A. E. *J. Phys. Chem.* **1959**, *63*, 1861-1868.

Table 3. Products and Branching Ratios of the Primary and Secondary Reactions between $C_{10}H_8^+$ and Atoms^a

O	$C_{10}H_8^+$ (128) ^b	→	$C_{10}H_8O^+$ (144)	[M] ^c	→	$C_{10}H_8O_2^+$ (160)	[M]	→	$C_{10}H_8O_3^+$ (176)	[M]
		0.45			0.2			0.2	$C_9H_7O_2^+$ (147)	[HCO]
					(0.1) ^e	$C_8H_6O^+$ (118)	[H ₂ C ₂ O]	0.8		
					0.4	$C_9H_8O^+$ (132)	[CO]	→	$C_8H_8O^+$ (120)	[CO]
								→	$C_8H_7O^+$ (119)	[HCO]
								→	$C_7H_5O^+$ (105)	[H ₃ C ₂ O] ^d
					→	$C_9H_7O^+$ (131)	[HCO]	0.4		
		→	$C_{10}H_7O^+$ (143)	[H]	0.3			0.4	$C_7H_8^+$ (92)	[CO]
		0.01			→	$C_9H_8O^+$ (132)	[M]	→	$C_7H_7^+$ (91)	[HCO]
		→	$C_9H_8^+$ (116)	[CO]	0.05			0.6		
		0.55			→	$C_9H_7O^+$ (131)	[H]			
					0.2					
					→	$C_8H_8^+$ (104)	[CO]			
					0.75					
N	$C_{10}H_8^+$ (128)	→	$C_{10}H_8N^+$ (142)	[M]						
		0.7								
		→	$C_9H_7^+$ (115)	[HCN]						
		0.3								
H	$C_{10}H_8^+$ (128)	→	$C_{10}H_9^+$ (129)	[M]						
		1.0								

^a Experiments done at 0.5 Torr of helium pressure. Accuracy of branching ratios is estimated to be $\pm 10\%$ for primary products and $\pm 30\%$ for secondary and tertiary products. ^b Mass of the ion in amu. ^c Neutral product; [M] represents three-body association. ^d Inferred from the nonreactivity of $C_9H_7O^+$ (m/z 131) and the good correlation with the $C_9H_8O^+$ peak (m/z 132) when varying the reaction time. This product at mass 105, bearing an oxygen atom, must be formed together with the neutral acetyl radical containing two carbon atoms; thus, this reaction probably cleaves one ring in the $C_9H_8O^+$ reactant. This is not in contradiction with the previous discussion on the indene structure, as in this case the reactant bears an oxygen atom on one ring, and consequently, during the reaction it is possible to form two stronger CO bonds in a concerted way. ^e May also arise from $C_9H_8O^+$ (m/z 132) + O \rightarrow $C_8H_6O^+$ + H₂CO. Inferred from analogy with $C_9H_8O^+$ + O \rightarrow $C_7H_5O^+$ + H₃C₂O. The reaction $C_{10}H_8O^+$ + O \rightarrow $C_8H_6O^+$ + H₂C₂O (ketene) is exothermic by more than 107 kcal/mol (Lias, S. G.; Bartmess, J. E.; Liebman, J. F.; Holmes, J. L.; Levin, R. D.; Mallard, W. G. *J. Phys. Chem. Ref. Data* **1988**, 17, Suppl. 1) if $C_{10}H_8O^+$ has an epoxy structure. This may be sufficient to open the ring. Alternatively, if the naphthalenol structure is chosen for $C_{10}H_8O^+$, the reaction will be exothermic by only ~ 50 kcal/mol, which is not sufficient to open the ring.

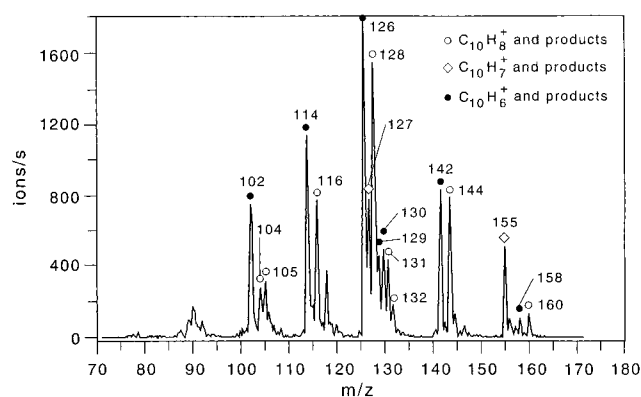


Figure 9. Combined spectrum of the reactions of $C_{10}H_6^+$, $C_{10}H_7^+$, and $C_{10}H_8^+$ with O atoms. $C_{10}H_6^+$ and $C_{10}H_8^+$ show the same reactivity with essentially the formation of the same neutral products, so the two spectra appear similar but shifted by 2 masses. $C_{10}H_7^+$ is unreactive with O, and the only reaction is association with N₂ to form a product at mass 155.

the ability of O atoms to make strong bonds with atomic carbon. For instance, in the case of anthraquinone, the reaction is rationalized as the breaking of a C–C bond to provide an additional electron to the carbon bearing the oxygen atom. This electron further participates in a new π -bond in CO, and the internal energy of the molecule is sufficient to break the remaining weakened C–C bond, thus allowing the carbonyl group to leave the molecule. The similarity of the mass spectra

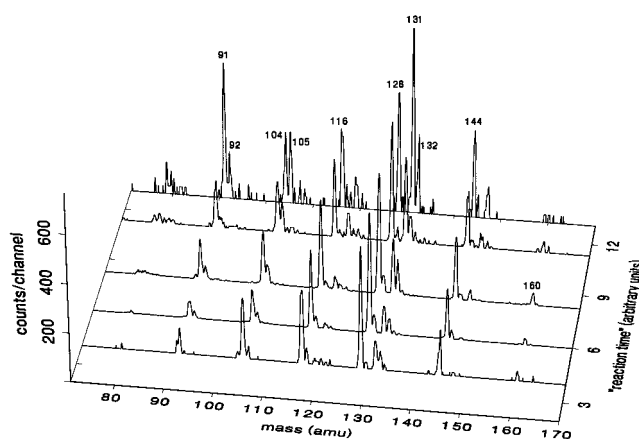


Figure 10. Spectra showing the reaction between $C_{10}H_8^+$ and O atoms at different pressures and flow rates of the helium carrier gas. At high pressure, the secondary products at masses 91 and 131 are the major peaks, due presumably to their lower reactivity accompanying the loss of their radical character.

of benzotropone $C_{11}H_8O$ and naphthalene $C_{10}H_8$ upon electron impact ionization has led these authors to infer that the remaining ion after ejection of the CO fragment in the case of benzotropone has the naphthalene structure, thus preferring a ring structure over a chainlike structure. However, it should be noted that recent studies have proven that different PAHs⁺ isomers have nearly identical fragmentation patterns, which suggests

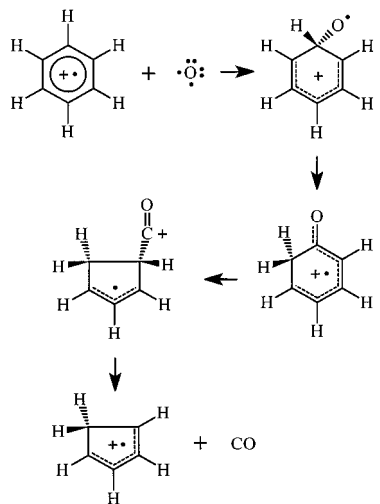
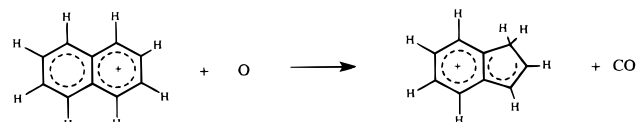


Figure 11. Proposed scheme for the reaction between benzene cation and O atoms.

isomerization prior to fragmentation,⁵⁷ and these unusually high dissociation thresholds for ionized PAHs allow them to access several isomeric forms.

We suggest a similar process in the case of the reaction $C_{10}H_8^+ + O \rightarrow C_9H_8^+ + CO$ with the formation of a hydrogenated ketone intermediate. We use this mechanism in the case of the reaction between benzene and O atoms as an example since benzene and naphthalene cations show similar behavior in their reaction with O atoms (see Figure 11). The first step is the addition of the triplet oxygen atom to the cation, followed by hydrogen atom transfer, and then ring contraction and loss of carbon monoxide. We can estimate the enthalpy of formation of the ketone if we assume the proton affinity of C_6H_5O to be comparable to the proton affinity of C_6H_6 and C_6H_5F ⁵⁸ (180.0 and 181.3 kcal/mol, respectively). The known enthalpy of formation of phenoxy radical then leads to a value of 196 kcal/mol for ΔH_f° ($C_6H_6O^+$). The product ion can have either the cyclopentadiene structure or the 1,2,4-pentatriene structure. Formation of pentatriene (or other related compounds such as 3-penten-1-yne, after rearrangement of the H atoms) requires the ring to be opened during the decarbonylation. Calculations at the ROMP2/6-31G*//ROHF/6-31G* level using the Gaussian 94 program package⁵⁹ show that this process requires about 140 kcal/mol in the most favorable configuration when the ring is opened near the carbon bearing the two H, and even more if the opening occurs elsewhere. This energy of activation makes the reaction $C_6H_6^+ + O \rightarrow l-C_5H_6^+ + CO$ endothermic by approximately 50 kcal/mol, and therefore the only available channel is the formation of the cyclopentadiene cation.

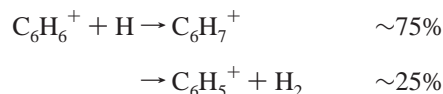
In the case of naphthalene, the reaction $C_{10}H_8^+ + O \rightarrow c-C_9H_8^+ + CO$ is exothermic by 82.7 kcal/mol. Thus, if the opening of the five-carbon ring in indene also requires about



140 kcal/mol, the reaction will be endothermic for the formation of 2-methylphenylacetylene, $l-C_9H_8^+$. Consequently, we favor the assignment of indene cation for the product of this reaction.⁶⁰ Table 3 shows a complete picture of the reactions for the $C_{10}H_8^+ + O$ system.

In the case of the reaction between $C_{10}H_8^+$ and N atoms, we can make a parallel with the corresponding benzene reaction, $C_6H_6^+ + N \rightarrow C_5H_5^+ + HCN$, which has an exothermicity of 62 kcal/mol for formation of cyclic $C_5H_5^+$. This relatively small exothermicity, compared to the energy needed for ring opening, causes us to favor a ring structure for $C_5H_5^+$, using the same reasoning as in the case of the reaction with O atoms. Additional evidence for a ring structure for the product $C_5H_5^+$ will be presented in the last section.

(ii) Reactions of $C_{10}H_n^+$ with H and D Atoms. Reaction of $C_{10}H_8^+$ with H atoms gives the adduct ion $C_{10}H_9^+$. An estimate of the H atom density was made using the reaction $CO_2^+ + H \rightarrow HCO^+ + O$.³³ CO_2^+ also reacts with H_2 to form HCO_2^+ . CO_2^+ was first injected into the reaction flow tube with a known flow of molecular hydrogen through the microwave discharge. Monitoring the HCO_2^+ signal at mass 45 with the discharge on and off allows us to estimate the production of H atoms by observing the decrease of the signal. $C_{10}H_8^+$ was then injected while maintaining the same H_2 flow and, therefore, the same H density when the discharge was on. Returning to the CO_2^+ calibration allows us to ensure that conditions were stable. We also employed another calibration reaction:



The H atom transfer is exothermic by 16 kcal/mol, while the association is exothermic by 81 kcal/mol.²⁶ We found approximately the same branching ratios as that determined by Scott et al.²⁷ These branching ratios were deduced by taking into account the saturated association reaction between $C_6H_5^+$ and H_2 ^{26,42} at various H_2 flows and extrapolation of the branching ratio to zero flow. The bimolecular reaction channel was not observed in the case of the naphthalene cation because either the reaction $C_{10}H_8^+ + H \rightarrow C_{10}H_7^+ + H_2$ is slightly endothermic or the complex is stabilized before entering the H abstraction channel. $C_{10}H_7^+$ was found to be less reactive, which is consistent with its lack of radical character. We report here an upper limit of about 5×10^{-11} cm³/s as no attempt was made to look selectively at the reactivity of both $l-C_{10}H_7^+$ and $c-C_{10}H_7^+$. The same comment applies to $C_{10}H_6^+$, which is found to be as reactive as $C_{10}H_8^+$. However, we can propose a hypothesis concerning the reactivity of this last species: it is probable that the radical and charge character of the acyclic species are confined in the benzene ring (as in 1,2-diethynyl benzene or 1-butadiene-benzene), and therefore reaction with

(60) Direct experiments on the reaction between indene cation and O atoms show that masses 104 and 91 are primary and secondary products, respectively, of this reaction. Four ways of producing $C_9H_8^+$ are used: from the mild ionization using chemical ionization with $C_6H_6^+$ to the strongest direct ionization with electrons at 50 eV; in addition, reactions with Ar^* and He^+ are also used. All four reactions give the same product and thus are not helpful in the assignment of the structure of the product at mass 116. However, this is consistent with a ring structure (indene cation) since the ionization using $C_6H_6^+$ and the Penning ionization with Ar^* are not sufficiently exothermic to open the ring.

(57) Pachuta, S. J.; Kentamaa, H.; Sack, T. M.; Cerny, R. L.; Tomer, K. B.; Gross, M. L.; Pachuta, R. R.; Cooks, R. G. *J. Am. Chem. Soc.* **1988**, *110*, 657–665.

(58) Szulejko, J. E.; McMahon, T. B. *J. Am. Chem. Soc.* **1993**, *115*, 7839–7848.

(59) Frisch, M. J.; Trucks, G. W.; Schlegel, H. B.; Gill, P. M. W.; Johnson, B. G.; Robb, M. A.; Cheeseman, J. R.; Keith, T. A.; Petersson, G. A.; Montgomery, J. A.; Raghavachari, K.; Al-Laham, M. A.; Zakrzewski, V. G.; Ortiz, J. V.; Foresman, J. B.; Cioslowski, J.; Stefanov, B. B.; Nanayakkara, A.; Challacombe, M.; Peng, C. Y.; Ayala, P. Y.; Chen, W.; Wong, M. W.; Andres, J. L.; Replogle, E. S.; Gomperts, R.; Martin, R. L.; Fox, D. J.; Binkley, J. S.; Defrees, D. J.; Baker, J.; Stewart, J. P.; Head-Gordon, M.; Gonzalez, C.; Pople, J. A. *Gaussian 94*; Gaussian Inc.: Pittsburgh, PA, 1995.

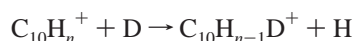
Table 4. Comparison between $C_{10}H_8^+$ and $C_6H_6^+$ Reactivities toward H_2 , H , O , and N^a

	reactant					
	c- $C_{10}H_8^+$	c- $C_6H_6^+$	c- $C_{10}H_7^+$	<i>l</i> - $C_{10}H_7^+$	c- $C_6H_5^+$	<i>l</i> - $C_6H_5^+$
H_2	<0.0005 ^b	<0.001 ^c	0.052 ^b	<0.001 ^b	0.05 ^c	<0.001 ^c
H	0.19 ^b	0.23 ^d	≤0.05 ^b	<0.01 ^c	<0.005 ^c	<0.005 ^c
O	0.1 ^b	0.095 ^b	<0.02 ^b	—	—	—
N	0.023 ^b	0.12 ^b	<0.01 ^b	—	—	—

^a Observed rate coefficients in units of $10^{-9} \text{ cm}^3 \text{ s}^{-1}$. Helium pressure is 0.5 Torr; association reactions are termolecular. ^b This work. The accuracy of the rate coefficients is estimated to be $\pm 50\%$ for reaction between c- $C_6H_6^+$ and N and O atoms; for the other reactions, the accuracy is reported in Tables 1 and 2. ^c Petrie, S.; Javahery, G.; Bohme, D. K. *J. Am. Chem. Soc.* **1992**, *114*, 9205–9206. The accuracy of the rate coefficients is estimated to be $\pm 50\%$ for reactions with H atoms and $\pm 30\%$ for reactions with H_2 . ^d Petrie, S.; Javahery, G.; Bohme, D. K. *J. Am. Chem. Soc.* **1992**, *114*, 9205–9206. Scott, G. B. I.; Fairley, D. A.; Freeman, C. G.; McEwan, M. J.; Adams, N. G.; Babcock, L. M. *J. Phys. Chem.* **1997**, *101*, 4973–4978. Accuracy estimated to be $\pm 30\%$.

H atoms may be as efficient as the reaction between $C_6H_6^+$ and H atoms. This might explain why $C_{10}H_6^+$ is slightly more reactive than $C_{10}H_8^+$, because its reactivity is closer to that of the benzene cation due to the presence of the *l*- $C_{10}H_6^+$ form.

We have also investigated the reactivity of $C_{10}H_9^+$, as this ion is produced efficiently in reactions between $C_{10}H_n^+$ and molecular and atomic hydrogen. The protonated naphthalene ion was produced in the source flow tube by the mildly exothermic, fast reaction $C_{10}H_8 + H_3O^+ \rightarrow C_{10}H_9^+ + H_2O$ to prevent ring opening. $C_{10}H_9^+$ is essentially unreactive with H atoms, and we report here a rate coefficient for the reaction between $C_{10}H_9^+$ and H of $4 \times 10^{-12} \text{ cm}^3/\text{s}$. Finally, exchange reactions between H and D atoms in $C_{10}H_6^+$, $C_{10}H_7^+$, and $C_{10}H_8^+$ of the form



were found to be slow, and the rate coefficients are lower than $10^{-11} \text{ cm}^3/\text{s}$ for all these processes.

Comparison between the Chemistry of Naphthalene and Benzene Cations. It is valuable to address a comparison between the chemistry of naphthalene and benzene cations. Table 4 shows the results of reactions with atoms and molecules for both of these ions. Due to the lack of measurements between $C_6H_6^+$ and O and N atoms, we have studied both of these reactions. $C_6H_6^+$ was found to react with O atoms in a manner very similar to that of $C_{10}H_8^+$; the main difference was the absence of the formation of adduct cation $C_6H_6O^+$. Since the reactions between O atoms and PAH cations are of importance from an astrophysical point of view, the measurement of the difference in reactivity of $C_6H_6^+$ relative to that of $C_{10}H_8^+$ was performed in the following way: the flow of O atoms was set to a known value, and then $C_6H_6^+$ was first selected and spectra were taken at different helium pressures (between 0.3 and 1.0 Torr); $C_{10}H_8^+$ was then selected and the same measurements were carried out (the O atom flow was kept constant during the experiment). Hence, we are certain that the contribution of wall loss, if any, was the same for the two cations. In both cases, the association reaction is exothermic by more than 100 kcal/mol, but the naphthalene cation is more likely to form a long-lived complex due to its greater number of degrees of freedom. This may explain why the adduct cation $C_6H_6O^+$ is not seen; the short-lived complex is likely to dissociate in a much shorter time than the collision time with the helium buffer. The reactions with O and N atoms lead to the formation of CO and HCN ,

and it is worth noting that it has been reported, while still the subject of some controversy, that CO possibly forms in the reaction between neutral benzene and $O(^3P)$ in a high-temperature, fast-flow reactor mass spectrometer.⁶¹ The striking fact, when looking at Table 4, is the very different behavior of reactions with N and O atoms on one hand and reactions with H atoms on the other hand in going from benzene to naphthalene cation. Apart from the fact that there is no H atom transfer in the case of naphthalene cation, there is a surprising similarity between the two systems: the rate coefficients are very similar for c- $C_6H_5^+$ and c- $C_{10}H_7^+$ with H and H_2 and for $C_6H_6^+$ and $C_{10}H_8^+$ with H atoms. Even the double dehydrogenation of $C_{10}H_6^+$ or the opened structure of *l*- $C_{10}H_6^+$ seem not to affect the reactivity in a significant way. The fact that the rates of reactions with H atoms are higher in the case of naphthalene cation relative to those of reactions with N and O could be partly due to formation of the strong CH bond, which may increase the complex lifetime.⁶²

Theoretical work indicates that larger PAHs are likely candidates for carriers of the DIBs. Theoretical studies of Du, Salama, and Loew⁶³ on the naphthalene cation and its hydrogen abstraction and addition derivatives suggest that $C_{10}H_9^+$ is not likely to absorb in the visible region of the spectrum due to the complete filling of the π bonding orbitals (this prevents visible transitions from lower π levels to the highest occupied π level to occur; therefore, only UV transitions $\pi \rightarrow \pi^*$ are accessible within the π system). However, the gap between the last π bonding orbital and the first π antibonding orbital becomes smaller as the size of the PAH increases; PAHs with more than 10 fused rings may absorb in the visible,⁶⁴ so the protonated forms of larger PAHs are possible carriers of the DIBs. It has been pointed out by Léger⁶⁵ that the abundance of PAHs needed to explain the diffuse bands is only about 1% of the quantity needed to explain the infrared emission features; this leads to the interesting possibility that, even if the protonated form is not absorbing in the visible, these species may lead to other closely related radical molecules and ions which are good candidates for absorption.

Generic Reactivity of PAH Cations Using the Curve-Crossing Model. In examining the chemistry of $C_{10}H_8^+$, $C_{10}H_7^+$, and $C_{10}H_6^+$, one can see that the reactivities of these ions show opposite patterns. While $C_{10}H_8^+$ and $C_{10}H_6^+$ react readily with atoms but not with molecules, $C_{10}H_7^+$ displays a high reactivity with molecules (up to about three-fourths of the collision rate with H_2O) and a low reactivity with atoms.

This behavior can be explained using the framework of valence bond theory and the curve-crossing model.^{66–68} In this qualitative, pictorial model, the electronic configurations of reactants and products are plotted along the x -axis, which represents the reaction coordinate, while the energies of these configurations are plotted along the y -axis, showing how the energy of each configuration is altered when the geometry changes during the reaction (see Figure 12). Of course, a single configuration is not sufficient to fully characterize the reactants or products, and there is certainly a mixing of additional

(61) Bajaj, P. N.; Fontijn, A. *Combust. Flame* **1996**, *105*, 239–241.

(62) Dunbar, R. C. *Int. J. Mass Spectrom. Ion Processes* **1997**, *160*, 1–16.

(63) Du, P.; Salama, F.; Loew, G. H. *Chem. Phys.* **1993**, *173*, 421–437.

(64) Salama, F.; Bakes, E. L. O.; Allamandola, L. J.; Tielens, A. G. G. M. *Astrophys. J.* **1996**, *458*, 621–636.

(65) Léger, A. In *The Diffuse Interstellar Bands*; Tielens, A. G. G. M., Snow, T. P., Eds.; Kluwer Academic Press: Dordrecht, The Netherlands, 1995; Vol. 202, pp 363–368.

(66) Pross, A. *J. Am. Chem. Soc.* **1986**, *108*, 3537–3538.

(67) Shaik, S. S.; Pross, A. *J. Am. Chem. Soc.* **1989**, *111*, 4306–4312.

(68) Pross, A. *Theoretical and Physical Principles of Organic Chemistry*; Wiley: New York, 1995.

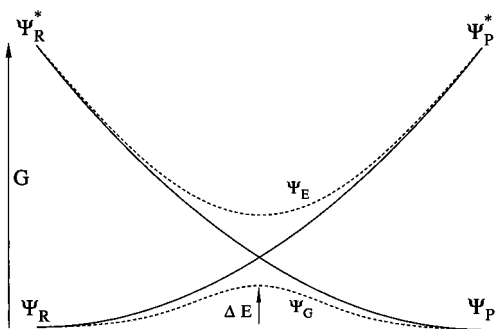


Figure 12. Curve-crossing model. ψ_R and ψ_P are the configurations which describe the reactants and the products. ψ_R^* and ψ_P^* are excited states belonging to the ψ_P and ψ_R configurations, respectively, but are distorted so that they have the same geometries as the reactants and products. The activation energy ΔE depends on the energy gap G between the two configurations at the reactants geometry. ψ_E (excited) and ψ_G (ground) are obtained from the mixing of the two configuration curves (Pross, A. *Theoretical and Physical Principles of Organic Chemistry*; Wiley: New York, 1995).

configurations to properly describe these two states; nevertheless, each configuration chosen on the diagram is close to the actual state of the molecule with respect to the bond-making/breaking process which the system undergoes during the reaction. As the molecular geometry is distorted in going from reactants to products, it may occur that the two respective configuration energy curves eventually cross each other. In this case, as the energies of the configurations become closer, a mixing takes place, leading to a generic avoided crossing of the two curves. The barrier of the reaction will depend on the position of the curve-crossing (a fraction f of the energy gap G between the reactants and products configuration at the reactants geometry) and the avoided crossing parameter B , which is the difference in energy between the point where the crossing occurs and the transition state at the top of the barrier below the crossing. Thus, the height of the barrier, ΔE , is given by

$$\Delta E = fG - B$$

where f and B are usually estimated to be about 0.2 and ~ 15 kcal, respectively.^{69,70} Consequently, a high value of G will lead to a slow reaction, if any, while a small value will lower the energy barrier, thus favoring the reaction.

In the case of naphthalene, most of the reactions can be rationalized as an electron shift process between a donor D and an acceptor A. For instance, using the case of $C_{10}H_7^+ + NH_3$ as an example, the reactant configuration will be $C_{10}H_7 \cdot NH_3^+$, where the nucleophile NH_3 has donated an electron to $C_{10}H_7^+$. Thus, in this case, the energy gap G at the frozen geometry of the reactants is equal to $I_v(NH_3) - EA(C_{10}H_7^+)$, where $I_v(NH_3)$ is the vertical ionization energy of NH_3 and $EA(C_{10}H_7^+)$ is the vertical electron affinity of the acceptor $C_{10}H_7^+$ (which we can estimate to be the same as the ionization potential of the $C_{10}H_7 \cdot$ neutral radical, an approximation which is known to be accurate within $\sim 10\%$). Now, in the case of the reaction between $C_{10}H_8^+$ and NH_3 , the situation is very different, since a single electron shift from NH_3 to $C_{10}H_8^+$ will merely generate the neutral $C_{10}H_8$, which does not describe the configuration of the product at the reactants geometry. In fact, the configuration which properly describes the reactants is that in which $C_{10}H_8$ is in the excited triplet state, $\cdot C_{10}H_8^*$ (if the C–N bond is distorted from the product geometry to the reactant geometry, the triplet $\cdot C_{10}H_8^*$

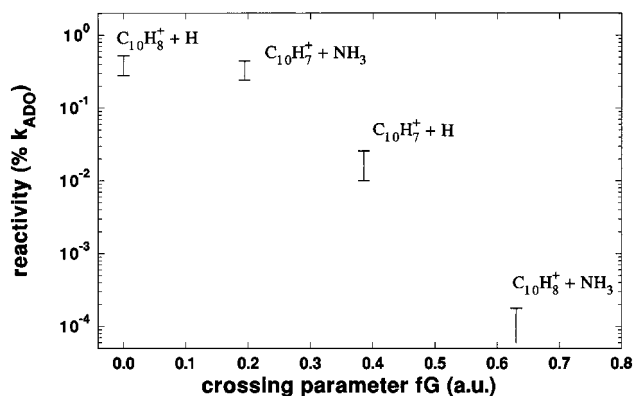


Figure 13. Efficiency of different types of reactions versus the energy parameter fG of the corresponding reactions. There is a clear correlation between the reactivity and fG (see text for details). In particular, the radical cation/radical and model cation/nucleophile reactions have much higher reactivities than the radical cation/nucleophile and model cation/radical reactions, in agreement with the curve-crossing model. Efficiencies are calculated using the ADO model (Su, T.; Bowers, M. T. In *Gas-Phase Ion Chemistry*; Bowers, M. T., Ed.; Academic Press: New York, 1979; Vol. 1, pp 83–118) for the collision rate. In the case of the radical/radical reaction $C_{10}H_8^+ + H$, the rate has been reduced to 25% of the collision rate (the proportion one would expect for the formation of a singlet product according to the Wigner–Witmer spin conservation rule) (Pearson, R. G. *Symmetry Rules for Chemical Reactions*; Wiley: New York, 1976). The vertical ionization energy for NH_3 was taken from the following: Aue, D. H.; Bowers, M. T. In *Gas-Phase Ion Chemistry*; Bowers, M. T., Ed.; Academic Press: New York, 1979; Vol. 2, p 16. The electron affinities of $C_{10}H_8^+$ and $C_{10}H_7^+$ have been replaced by the ionization potential of the parent neutrals. The ionization potential of $C_{10}H_7 \cdot$ has been estimated from the value for $C_{10}H_8$ and a correction factor from the known ionization potentials of the couple phenyl radical/benzene; enthalpies of reactions are calculated or estimated from the literature (Lias, S. G.; Bartmess, J. E.; Liebman, J. F.; Holmes, J. L.; Levin, R. D.; Mallard, W. G. *J. Phys. Chem. Ref. Data* **1988**, *17*, Suppl. 1). The vertical singlet–triplet splittings $\Delta E_{\pi-\sigma}$ for $C_{10}H_7^+$ and $C_{10}H_8$ were calculated using the Gaussian 94 program package or found in the literature (McGlynn, S. P.; Azumi, T.; Kinoshita, M. *The Triplet State*; Prentice Hall: Englewood Cliffs, NJ, 1969).

and the ammonia cation NH_3^+ will be formed). Consequently, the energy gap G is equal to $I_v(NH_3) - EA(C_{10}H_8^+) + \Delta_{ST}$, where Δ_{ST} is the singlet–triplet excitation of the neutral $C_{10}H_8$. As the energy barrier is directly connected to the value of G , one can see that the reaction between $C_{10}H_8^+$ and NH_3 will be much less favorable than the corresponding reaction, $C_{10}H_7^+ + NH_3$. Similarly, for the reaction $C_{10}H_8^+ + \cdot H$, which is a radical/radical reaction, we expect the energy barrier to be nonexistent, or at least very small, while for the reaction $C_{10}H_7^+ + \cdot H$ the product $C_{10}H_8^+$ must lead to a triplet cation $\cdot C_{10}H_7^+$ at the reactant geometry, therefore increasing the energy barrier. Figure 13 shows a plot of the efficiencies of reactions versus the energy parameter fG for each kind of reaction. The parameter fG (the barrier height of the curve-crossing in Figure 12) is linked to the activation energy and thus to the reactivity. This parameter depends primarily on the energy gap G and on the exothermicity of the reaction. The calculation assumes a parabolic shape for the configuration curves and a constant value of 60 kcal/mol for the difference in energy between ψ_R and ψ_P^* (any value between 0 and 100 kcal/mol gives the same qualitative result). The reactivity of $C_{10}H_7^+$ toward H atoms, for example, is enhanced by the high exothermicity of the reaction (~ 100 kcal/mol), thus giving a higher efficiency than one would expect for a reaction between a model cation and

(69) Buncel, E.; Shaik, S. S.; Um, I. K.; Wolfe, S. *J. Am. Chem. Soc.* **1988**, *110*, 1275–1279.

(70) Shaik, S. S. *J. Org. Chem.* **1987**, *52*, 1563–1568.

atom. In contrast, the $C_{10}H_8^+ + NH_3$ reaction, which is mildly exothermic with a high gap, has a very low efficiency.

To summarize the argument, the lowering of the reactivity between $C_{10}H_8^+$ and NH_3 with respect to that of $C_{10}H_7^+ + NH_3$ is due to the existence of a doubly excited product in the first case, while the products are only singly excited in the second case. Similarly, the difference in reactivity of $C_{10}H_8^+$ and $C_{10}H_7^+$ toward atoms lies in the higher excitation of $C_{10}H_7^+$ necessary to form the products in the correct configuration.

This qualitative model emphasizes the role of the state of the cation and shows qualitatively that the chemistries of singlets and multiplets are expected to be very different. This further confirms our findings that the products of the reaction between $C_{10}H_8^+$ and N are unreactive because they are in a singlet state, while the reaction $C_{10}H_8^+ + \bullet O \bullet$ leads to a variety of secondary products, which are radicals like the parent cation. The low reactivity of $C_6H_5^+$ and $C_{10}H_7^+$ with atoms argues for a singlet state for these cations, which is supported by our calculations of singlet–triplet splittings. These calculations are in good qualitative agreement with the experimental lack of reactivity of $C_6H_5^+$ and $C_{10}H_7^+$, which is thus seen as the manifestation of a singlet state.⁷¹ Similarly, our calculations of the singlet–triplet splittings for the cyclopentadienyl cation $C_5H_5^+$ and the dehydrogenated pyrene cation $C_{16}H_9^+$ indicate that these ions have triplet ground states.⁷¹ This result is consistent with the high reactivity of these ions.

It is worth noting that $C_5H_5^+$, the primary product of the reaction between $C_6H_6^+$ and N atoms, reacts further with N. It is thus highly probable that $C_5H_5^+$ has a triplet ground state (unlike the corresponding singlet product in the naphthalene

case), which allows further reaction with N to give the doublet $C_4H_4^+$ and, finally, the unreactive terminal cyclopropenyl aromatic cation $C_3H_3^+$, which is a singlet. This experimentally observed chain of spin-allowed reactions between $C_6H_6^+$ and N atoms can be regarded as additional evidence for a cyclic form for the product between PAHs⁺ and atoms because $C_5H_5^+$, in linear form, is not believed a priori to have a triplet ground state, while the *c*- $C_5H_5^+$ cyclopentadienyl cation is known experimentally to be a triplet ground-state cation.^{72–74}

Conclusion

The rapid addition of hydrogen atom to $C_{10}H_8^+$ and to $C_{10}H_6^+$, as well as the facile radiative association of molecular hydrogen to $C_{10}H_7^+$, indicates that protonated naphthalene will be a terminal ionic species in interstellar environments where the naphthalene cation and its derivatives are able to survive. Comparisons with the reactions of benzene suggest that similar conclusions can be drawn for other aromatic systems. A detailed discussion of the astrophysical implications of this work will be presented in a separate publication. Finally, we have reported here novel reaction pathways for naphthalene cation with O and N atoms, where the reactions proceed through C and CH abstraction without cleavage of the ring structure.

Acknowledgment. We gratefully acknowledge support of this research by the National Aeronautics and Space Administration. We appreciate sponsorship of the computational studies by the National Science Foundation (CHE-9734867).

JA983472A

(71) If $C_{10}H_7^+$ were a triplet ground-state cation, the expected rate constant would be about one-third of the collision rate and, therefore, more than the corresponding rate coefficient for the $C_{10}H_8^+ + H$ reaction (one-fourth of k_{coll} due to the spin conservation law). The same argument applies to $C_6H_5^+$. Further evidence on the pyrenium triplet cation is presented in the following: Le Page, V.; Keheyan, Y.; Snow, T. P.; Bierbaum, V. M. *Int. J. Mass Spectrom.* **1999**, 185/186/187, 949–959.

(72) Pearson, R. G. *Symmetry Rules for Chemical Reactions*; Wiley: New York, 1976.

(73) Aue, D. H.; Bowers, M. T. *Gas-Phase Ion Chemistry*; Academic Press: New York, 1979; Vol. 2.

(74) Saunders, M.; Berger, R.; Jaffe, A.; McBride, J. M.; O'Neill, J.; Breslow, R.; Hoffman, J. M.; Perchonok, C. J.; Wasserman, E.; Hutton, R. S.; Kuck, V. J. *J. Am. Chem. Soc.* **1973**, 95, 3017–3018.